

Entanglement properties of topological color codes

M. Kargarian*

Physics Department, Sharif University of Technology, Tehran 11155-9161, Iran

(Dated: March 5, 2019)

The entanglement properties of a class of topological stabilizer states, the so called two-dimensional *topological color codes* or 2-colex, are calculated. The topological entropy is used to measure the entanglement of different bipartitions of the 2-colex. The dependency of the ground state degeneracy on the genus of the surface shows that the color code can support a topological order, and the contribution of the color in its structure makes it interesting to compare with the Kitaev's toric code. While a qubit is maximally entangled with rest of the system, two qubits are no longer entangled showing that the 2-colex is genuinely multipartite entangled. For a convex region, it is found that entanglement entropy depends only on the degrees of freedom living on the boundary of two subsystems. The boundary scaling of entropy is supplemented with a topological subleading term which for a 2-colex defined on a compact surface is twice than the toric code. From the entanglement entropy we construct a set of bipartitions in which the diverging term arising from the boundary term is washed out, and the remaining non-vanishing term will have a topological nature. Besides the 2-colex on the compact surface, we also analyze the entanglement properties of a version of color code with border, i.e *triangular color code*.

PACS numbers: 03.67.-a, 03.67.Lx, 03.67.Mn

I. INTRODUCTION

In quantum information theory and quantum computations, entanglement is recognized as an essential resource for quantum processing and quantum communications, and it is believed that the protocols based on the entangled state has an exponential speed-up than the classical ones. Besides, in highly correlated state in condensed matter systems such as superconductors^{1,2}, fractional quantum Hall liquids³, the entanglement serves as a unique measure of quantum correlations between degrees of freedom. In quantum many-body systems such as spin, fermion and boson systems, the entanglement connected to the phase diagram of the physical system. Non-analytic behavior of entanglement close to the quantum critical point of the system and occurrence of finite size scaling provided an intense research leading to fresh our insight of the critical properties from the quantum information side, for a review see the review by L. Amico, *et al.*⁴ and references therein. In the past years the appearance of new phases of matter has intensified the investigation of the entanglement in the quantum systems. These are phases beyond the Landau-Ginzburg-Wilson paradigm⁵ where an appropriate local order parameter characterizes different behaviors of two phases on either side of the critical point. These phases of matter carries a kind of quantum order called *topological order*⁶ and the transition among various phases does not depend on the symmetry breaking mechanism. Therefore the Landau theory of classical phase transition fails in order to describe these phases. Ground state of such phases is a highly entangled state and the excitations above the ground state have a topological nature which mirrored in their exotic statistics.

Among the models with topological properties, the Kitaev or toric code⁷ has been extensively studied.

Ground state degeneracy depend upon the genus or handles of the manifold where the model is defined on, and there is a gap which separated the ground state subspace from the excited states. The ground state degeneracy can not be lifted by any local perturbations which underlines the Kitaev's model as a testground for fault-tolerant quantum computations⁷. The ground state of the Kitaev's model is indeed stabilized by group generated by a set of local operators called *plaquette* and *star operators* making it useful as a quantum error correcting code⁸. The information is encoded in the ground state subspace which is topologically protected such as quantum memory⁹. For this model any bipartition of the lattice has non-zero entanglement which manifests the ground state is generically multipartite entangled¹⁰. Bipartite entanglement scales with the boundary of the subsystem showing that the entanglement between two parts of the system depend only on the degrees of freedom living on the boundary which is a manifestation of the holographic character of the entanglement entropy¹¹.

For topological models a satisfactory connection between topological order and entanglement content of a model with topological properties has been established via introducing the concept of the *topological entanglement entropy* (*TEE*)^{12,13} which is a universal quantity with topological nature.

Another resource with topological protection character is called *color code*. An interplay between color and homology provides some essential features, for example a particular class of two-dimensional color codes or 2-colex with colored borders will suppress the need for selective addressing to qubits and whole Clifford group can be done¹⁴. The number of logical qubits which are encoded by a two dimensional color code are twice than the toric

code¹⁵ defined on the compact surface.

In this paper we study the entanglement properties of a two-dimensional color code, the so called 2-colex¹⁶. We consider different bipartitions of the lattice the model defined on and evaluate the entanglement entropy between them. The connection between the topological nature of the code and the entanglement entropy is also discussed. The structure of the paper is as follows. In sec(II) the basic notion of a color code on the surface has been introduced. In sec(III) base on the stabilizer structure of the protected code space the reduced density matrix which is needed for evaluating the entanglement entropy has been calculated. Then in sec(IV) the entanglement entropy for different bipartitions is calculated. In sec(V) another class of color code on plane and its entanglement properties are introduced, and the final section (VI) has been devoted to the conclusions.

II. PRELIMINARIES ON TOPOLOGICAL COLOR CODE

In this paper we consider a class of topological quantum error-correction code defined on the lattice, the so called topological color codes¹⁴. The local degrees of freedom are spin-1/2 with the bases of the Hilbert space C^2 . The lattice we consider composed of vertices, links and plaquettes. Each vertices stand for a local spin and ended with three links, and no two plaquettes with same color share the same link. We suppose this color structure is denoted by the notation $TCC\{V, E, P\}$ where the V, E, P denote the set of vertices, edges and plaquettes, respectively. For simplicity we define the model on the regular hexagonal lattice on the torus, i.e imposing periodic boundary conditions as shown in Fig.(1). There is subspace $\mathcal{C} \subset \mathcal{H}$ which is topologically protected. The full structure of this subspace and its properties is determined by definition of stabilizer group. the stabilizer group is generated by a set of plaquette operators. For each plaquette we adhere the following operators which are products of a set of Pauli operators of a vertices around a plaquette:

$$\Omega_p^C = \bigotimes_{v \in p} \Omega_v^C ; \quad \Omega = X, Z, \quad C = \text{Red, Green, Blue} \quad (1)$$

For a generic plaquette, say blue plaquette P_1 in Fig.(1) we can identify green and red strings which are the boundary of the plaquette. It is natural to think of product of different plaquette operators which may produce a collection of boundary operators. For example as is shown in Fig.(1) the product of two neighboring plaquettes, say red and blue ones, correspond to a green string P_2 which is a boundary of two plaquettes. All of string operators produced in this way commute with each other and with plaquettes since they share either nothing or even number of vertices. In addition to closed boundary operators, there are other closed string which are no longer the product of the plaquette operators. These

closed string form the fundamental cycles of the manifold in which the lattice is defined on and have a character of color. Number of these closed loops depends on the genus of the topological surface. For the torus with $g = 1$ there are two such cycles which are noncontractible loops in contrary to the closed boundary strings which are homotopic to the boundary of a plaquette. For the topological color codes these noncontractible loops are shown in Fig.(1). For every homology class of the torus there two closed string each of one color, say red and blue. Note that a generic string, say green, can be produced by the production of the red and blue strings when they are suitably chosen. In fact when two string meet the same vertex leave it invariant. Indeed there is an interplay between color and homology class of the model. One can define the nontrivial closed string as following:

$$\mathcal{S}_\mu^{C\Omega} = \bigotimes_{i \in I} \Omega_i \quad (2)$$

where I indexed the set of spins the generic string contains, μ stands for the homology class of the torus and Ω is the X or Z Pauli spin operator. Closed noncontractible loops turn on to form bases for the topological code. clarifying this, we label different loops as:

$$\begin{aligned} X_1 &\longleftrightarrow \mathcal{S}_2^{RX}, X_2 \longleftrightarrow \mathcal{S}_1^{BX}, X_3 \longleftrightarrow \mathcal{S}_2^{BX}, X_4 \longleftrightarrow \mathcal{S}_1^{RX} \\ Z_1 &\longleftrightarrow \mathcal{S}_1^{BZ}, Z_2 \longleftrightarrow \mathcal{S}_1^{RZ}, Z_3 \longleftrightarrow \mathcal{S}_1^{RZ}, Z_4 \longleftrightarrow \mathcal{S}_2^{BZ} \end{aligned} \quad (3)$$

These operators form a 4-qubit algebra in \mathcal{H}_2^4 , so it manifests a 16-dimensional structure for the coding space which is topologically protected. Now we move to construct the explicit forms of the states of the subspace \mathcal{C} . The above construction for the string operators in Eq.(3) can be extended to an arbitrary manifold with genus g . For such manifold the coding space spanned with 2^{4g} vectors. Note that for toric code (white and dark code)¹⁵ when is embedded in the same manifold with genus g , the coding space will span with 2^{2g} vectors¹⁰ which explicitly shows that the color codes have richer structure than the toric codes¹⁵.

A. Stabilizer Formalism

The protected subspace \mathcal{C} is spanned by the state vectors which are stabilized by some stabilizing group, i.e. a subset of Pauli group. Let \mathcal{U} be a set of generators of the stabilizer group and its elements are denoted by \mathcal{M} . So this subspace is:

$$\mathcal{C} = \text{Span}\{|\psi\rangle : \quad \mathcal{M}|\psi\rangle = |\psi\rangle \quad \forall \mathcal{M} \in \mathcal{U}\} \quad (4)$$

Let G be the group constructed by the generators of spin-flip plaquettes operators, i.e X_p^C . The cardinality of

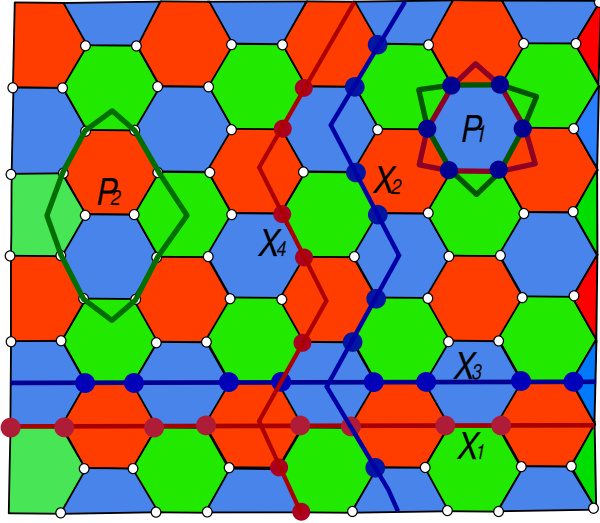


FIG. 1: (color online) topological color code defined on the hexagonal lattice with periodic boundary conditions. A hexagon (P_1), say blue, can be denoted by either red or green closed boundary string. Production of two neighboring plaquettes, say red and blue corresponds to a green string (P_2). Non-contractible loops (X_1, X_2, X_3, X_4) for topological color codes which determine different topological sectors of the color code are also depicted.

the group is then $|G| = 2^{|P|-2}$ where $|P|$ stand for the total number of the plaquettes. Note that all plaquettes are not independent since the product of all plaquettes of the same color represents the same action in the group, namely: $\prod_R X_p^C = \prod_B X_p^C = \prod_G X_p^C = X^{\otimes |V|}$. By starting from an initial vacuum state, say $|0\rangle^{\otimes |V|}$ where $Z|0\rangle = |0\rangle$, one can construct a state vector in the Hilbert space which is stabilized by the group elements. this state vector contains an equal superposition of the some bases of the Hilbert space. From the previous arguments, it is convenient to denote it by $|0000\rangle$ and has the form:

$$|0000\rangle = |G|^{-1/2} \sum_{g \in G} g|0\rangle^{\otimes |V|} \quad (5)$$

where the g is an element of the stabilizing group, i.e $g = \bigotimes_{p \in P} X_p^{r_p}$ where $r_p = 0(1)$ corresponds to the plaquette operator X_p appearing (not appearing) in the element group g . Considering the noncontractible loops, the stabilizer group can be extended. We denote it by $\bar{G} = \mathcal{A}.G$ where the group \mathcal{A} composed of different combination of noncontractible loop operators, i.e :

$$\mathcal{A} = \left\{ \prod_{\mu=1, C=B,R}^{\mu=4g} (S_\mu^{CX})^{r_s} \ , \ r_s = 0, 1 \right\} \quad (6)$$

The group \bar{G} is infact the centralizer with elements which commute with stabilizer group but not containing

in it, this means that the normal subgroup G divide the group \bar{G} into 2^{4g} cosets, i.e:

$$\bar{G} = \left\{ \prod_{\mu=1, C=B,R}^{\mu=4g} (S_\mu^{CX})^{r_s} . G \ , \ r_s = 0, 1 \right\} \quad (7)$$

The cardinality of group will be $|\bar{G}| = 2^{|P|+4g-2}$. Therefore the protected subspace \mathcal{C} is spanned by 2^{4g} states which correspond to different cosets. For the states of the stabilizer subspace we have, by construction:

$$\mathcal{C} = \text{Span}\{ |ijkl\rangle : |ijkl\rangle = X_1^i X_2^j X_3^k X_4^l |0000\rangle \} \quad (8)$$

where X_1, X_2, X_3, X_4 are defined in Eq.(3) and $i, j, k, l = 0, 1$. These topological non-trivial string operators can mapp the states of the coding space on to each other, and any error of this type will not be detectable. A generic state can be a superposition of different vectors of coding space:

$$|\Psi\rangle = \sum_{i,j,k,l} a_{i,j,k,l} |ijkl\rangle \ , \ \sum_{i,j,k,l} |a_{i,j,k,l}|^2 = 1 \quad (9)$$

B. Protected Subspace as a Ground State Subspace

From the practical point of viwe it is important to find a state of quantum many-body system for implementation of the univesal quantum computation. We can provide a construction in which the protected subspace be the ground sate of a Hamiltonian with local nature¹⁷. As for the structure of the stabilizer subspace, the subspace \mathcal{C} is the ground state of the exactly solvable Hamiltonian as:

$$H = - \sum_{p \in P} X_p - \sum_{p \in P} Z_p \quad (10)$$

The ground state of this Hamiltonian is 2^{4g} -fold degenerate and topologically protected from local errors. Different stats of the ground state subspace as it clear from Eq.(8) have a colored structure, say a red one may be constructed by the either \mathcal{S}_1^{RX} or \mathcal{S}_2^{RX} and a green one by applying $\mathcal{S}_1^{RX} . \mathcal{S}_1^{BX}$. An excited state will arise when the any of the stabilizing conditions in Eq.(4) violated. In energy units which the Hamiltonian in Eq.(10) has been defined, the first excite state will separated from the ground state by a gap of value 2.

III. REDUCED DENSITY MATRIX AND VON NUMANN ENTROPY

In this section we turn on to calculate the entanglement properties of the topological color codes. We consider a

generic bipartition of the system into subsystems A and B . Let Σ_A and Σ_B to be the number of plaquettes operators acting solely on A and B , respectively, and let Σ_{AB} to be stand for the number of plaquettes acting simultaneously on A and B , i.e these are boundary operators. We focus on the entanglement entropy between two partitions A and B of the code. To this end first the reduced density operator of the one subsystem has been evaluated and then the entanglement entropy is measured. The reduced density matrix for subsystem, say A , for a state in an equal superposition of the elements of group G has the following form¹⁰:

$$\rho_A = \frac{d_B}{|G|} \sum_{g \in G/G_B, \tilde{p} \in G_A} g_A |0_A\rangle \langle_A 0| g_A \tilde{g}_A \quad (11)$$

where G_A and G_B are subgroup of G which act trivially on subsystems B and A , respectively and d_A and d_B are their cardinality. So the von-Numman entropy is:

$$S_A = \log_2 |G_{AB}| \quad (12)$$

where $G_{AB} = \frac{G}{G_A G_B}$. It is a simple task to show that the entropy for all states of the coding space have the same entanglement entropy. To this end let $X(t) = X_1^i X_2^j X_3^k X_4^l$ where $t = (i, j, k, l)$ is a binary vector. So for a generic state in the coding space we have: $|t\rangle = X(t)|0\rangle$. Moreover the string operators $X(t)$ can be decomposed as: $X(t) = X(t)_A \otimes X(t)_B$, therefore:

$$\rho_A(|t\rangle) = \text{Tr}_B(|t\rangle\langle t|) = \text{Tr}_B(X(t)|0\rangle\langle 0|X(t)) = X(t)_A \text{Tr}_B(|0\rangle\langle 0|)X(t)_A = X(t)_A \rho_A(|0\rangle)X(t)_A \quad (13)$$

Hence by using the ancilla $S_A(t) = \lim_{n \rightarrow 1} \partial_n \text{Tr}[\rho_A^n]$, the entanglement entropy for a state $|t\rangle$ reads: $S_A(t) = S_A(0)$.

IV. ENTANGLEMENT OF TCC FOR VARIOUS BIPARTITIONS

In this section we design different spin configurations as a subsystem and then evaluate its entanglement with its complementary.

A. One Spin

As first example we consider the entanglement between one spin and remaining ones of the lattice. In this case there is no closed boundary operators acting exclusively on the spin, i.e subsystem A . So the reduced density matrix ρ_A is diagonal as follows:

$$\rho_A = f^{-1} \sum_{g \in G/G_B} g_A |0_A\rangle \langle_A 0| g_A \quad (14)$$

where $f = |G/G_B|$ is the number of operators which act freely on the subsystem A . As it is clear there are three plaquette operators which act freely on one spin since every spin in the color code is shared by the three plaquettes Fig.(1) and this leads to $f = 2^3 = 8$. Only half of operators of quotient group leading to the flipping of the spin. They will have trivial effect unless three plaquettes act either individually or altogether. Therefore the reduced density matrix is:

$$\rho_A = \frac{1}{2}(|1_A\rangle\langle_A 1| + |0_A\rangle\langle_A 0|) \quad (15)$$

Therefore in topological color code every spin is maximally entangled with other spins. For the surface code (Kitaev model) a single spin is also maximally entangled with other spins¹⁰.

B. Two Spins

We calculate the entanglement between two spins. For this case also there is not any closed boundary operator with nontrivial effect on two spins, so the reduced density matrix reads:

$$\rho_A = \frac{1}{4}(|11\rangle\langle 11| + |10\rangle\langle 10| + |01\rangle\langle 01| + |00\rangle\langle 00|) \quad (16)$$

The entanglement between two spins which is measured by the Concurrence¹⁸ vanishes. While each spin is maximally entangled with others, two spins are not entangled which is a manifestation that the topological color code is genuinely multipartite entangled like the surface codes.

C. Colored Spin Chain

In this case we aim to know how much a closed colored spin chain winding the torus nontrivially, say blue or red in Fig.(1) is entangled with rest of the code. For the sake of clarity and without loss of generality we consider a hexagonal lattice with $|P| = 3k \times 4k$ plaquettes, where

k is an integer number as 1, 2, 3..., for example in Fig.(1) $k = 2$. This choice makes the color code more symmetric. So the number of plaquettes with special color, say red, is $(2k)^2$, and the number of spins that the colored chain contains is $4k$. Let the system be in the $|0000\rangle$. For this state there is not any closed boundary which exclusively acts on the chain. Therefore the reduced density matrix is diagonal and the number of plaquette operators which act independently on the subsystem B is as follows:

$$\Sigma_B = (|P| - 2) - (3 \times 2k) + (2k + 1) \quad (17)$$

where the third term is the number of constraints on the plaquette operators acting on spin chain. In fact these are collective operators, i.e. product of boundary plaquette operators between A and B which act solely on B . With this remark the entanglement entropy becomes:

$$S_A = \log \frac{|G|}{d_B} = 4k - 1 \quad (18)$$

It is instructive to compare the obtained entanglement entropy in Eq.(18) with the entanglement of the spin chain in the Kitaev's model. For the latter case when the model defined on the square lattice on a compact surface, i.e. torus, there exists a rather similar scaling with the number of qubits living in the chain¹⁰. In both cases the entanglement entropy in Eq.(18) can be understood from the fact that only configurations with even number of spin flips of the chain allow in the ground state structure. Plaquettes which are free to act on the spin chain only able to flip even number of spins of the chain. The same arguments can be applied for other ground states $|ijkl\rangle$ where for all of them the entanglement entropy is given by Eq.(18). By inspection of other ground states we see that there are $2^3 = 8$ states in which in the spin chain the even number of spins have been flipped. These states are:

$$|0000\rangle, |X_1 0000\rangle, |X_3 0000\rangle, |X_4 0000\rangle, |X_1 X_3 0000\rangle$$

$$|X_1 X_4 0000\rangle, |X_3 X_4 0000\rangle, |X_1 X_3 X_4 0000\rangle \quad (19)$$

Besides there are $2^3 = 8$ states with an odd number of spin flipped for the spin chain which has been listed below:

$$|X_2 0000\rangle, |X_2 X_1 0000\rangle, |X_2 X_3 0000\rangle$$

$$|X_2 X_4 0000\rangle, |X_2 X_1 X_3 0000\rangle, |X_2 X_1 X_4 0000\rangle$$

$$|X_2 X_3 X_4 0000\rangle, |X_2 X_1 X_3 X_4 0000\rangle \quad (20)$$

Now we consider a generic state and calculate the entanglement entropy between the colored spin chain and rest of the lattice. The density matrix $\rho = |\Psi\rangle\langle\Psi|$ is:

$$\rho = \sum_{ijkl, mnpq} a_{ijkl} \bar{a}_{mnpq} X_1^i X_2^j X_3^k X_4^l \rho_0 X_1^m X_2^n X_3^p X_4^q \quad (21)$$

With the explanations we made above the eigenvalues of the reduced density matrix ρ_A for the even number of spin flipped is as follows:

$$\begin{aligned} \frac{d_B}{|G|} (|a_{0000}|^2 + |a_{1000}|^2 + |a_{0010}|^2 + |a_{0001}|^2 + |a_{1010}|^2 \\ + |a_{1001}|^2 + |a_{0011}|^2 + |a_{1011}|^2) = \frac{d_B}{|G|} \alpha \end{aligned} \quad (22)$$

where $\frac{|G|}{d_B} = 2^{4k-1}$. Note that the number of these eigenvalues is 2^{4k-1} . Through the similar arguments we see that the eigenvalues of reduced density matrix for odd spin flipped of the spin chain is: $\frac{d_B}{|G|} (1 - \alpha)$ with 2^{4k-1} for its number. So we can calculate the entanglement entropy as follows:

$$S_A = - \sum_{i=1}^{2^{4k}} \lambda_i \log \lambda_i = -2^{4k-1} \frac{d_B}{|G|} \alpha \log \frac{d_B}{|G|} \alpha - 2^{4k-1} \frac{d_B}{|G|} (1 - \alpha) \log \left(\frac{d_B}{|G|} (1 - \alpha) \right) = 4k - 1 + H(\alpha) \quad (23)$$

where $H(x) = -x \log x - (1 - x) \log(1 - x)$.

D. Red Strings Crossing

As another bipartition we select all spins carrying by the two red strings of different homologies, say $X_1 - X_4$ in Fig.(1), which have $2 \times 4k = 8k$ spins. Let system be in the $|0000\rangle$ state. There is not any closed boundary

operator acting solely on A . Considering the total number of independent plaquettes acting solely on subsystem B , the entanglement entropy then reads:

$$S_A = 8k - 1 \quad (24)$$

Again we see that there are only configurations with an even number of spin flipped in the construction of the state $|0000\rangle$. For a generic state such as Eq.(21) where we can realized all states with either even or odd number of spin flips, the entanglement entropy will be:

$$S_A = 8k - 1 + H(\alpha) \quad (25)$$

E. Red and Blue strings crossing

By this partition we mean that the $X_1 - X_2$ strings in Fig.(1). the subsystem A contains $8k - 1$ spins and again there is no closed boundary acting on. Enumerating the independent plaquettes operators acting on the subsystem B , the entanglement entropy is as follows:

$$S_A = 8k - 3 \quad (26)$$

F. Two Parallel Spin Chain

Two parallel spin chains, say red and blue ($X_1 - X_3$) in Fig.(1) or equivalently a green string, contain $2 \times 4k = 8k$ spins and again there is not any closed string acting on it nontrivially. $8k$ plaquettes act freely on subsystem A , but there are some constraints on them which arise from the product of plaquettes in which leave the subsystem A invariant and makes collective operator which acts solely on B . The product of blue and green plaquettes of those plaquettes which are free to act on A will produce a red string leaving A invariant. The same product hold for the red and green plaquettes. So the entanglement entropy reads:

$$S_A = 8k - 2 \quad (27)$$

Indeed this is entanglement entropy for a green string. However the number of spins it contains is twice than the strings we discussed in Subsec(C).

G. Spin Ladder

A set of vertical spin ladders has been shown in Fig.(2). In this subsection only one of them has been considered as subsystem A . Let the system be in the state $|0000\rangle$. In this case the subsystem A contains $2 \times 3k$ spins, and the total number on independent plaquettes acting on

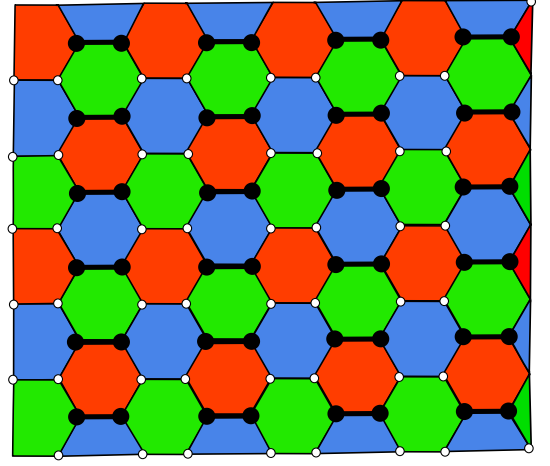


FIG. 2: (color online) A set of spin ladders on topological color code.

subsystem B is: $(|P| - 2) - 3 \times 3k + 3k$. Since there are not any closed string solely acting on A the entanglement entropy reads:

$$S_A = 6k \quad (28)$$

So it is clear that this spin ladder has maximum entanglement with the rest of the system and its state turns the maximum mixing, namely:

$$\rho_A = 2^{-6k} \mathbf{I}_{6k \times 6k} \quad (29)$$

H. Vertical Spin Ladders

A set of vertical spin ladders has been depicted in Fig.(2) and again we suppose the system is in the state $|0000\rangle$. Although there are no any plaquette which acts solely on subsystem A , there are some products of them producing closed string in which that act solely on A . Both subsystems A and B are symmetric with respect to each other. So the number of closed strings which act only on A and B will be: $d_A = d_B = 2^{2k}$. Finally the entanglement entropy reads:

$$S_A = 12k^2 - 4k - 2 \quad (30)$$

I. A Hexagonal Disk

In this case we adapt a situation in which a set of plaquettes intuitively form a hexagon as shown in Fig.(3). In this figure the dashed hexagon demonstrates the set of plaquettes between two subsystems. We suppose that

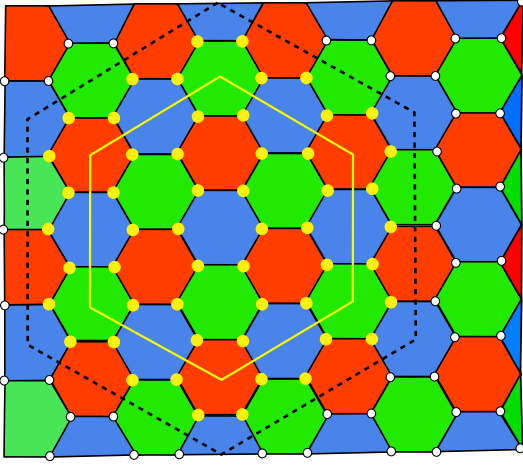


FIG. 3: (color online) A manifestation of a hexagonal disk. a set of plaquettes are chosen in such way that form a hexagon (the yellow hexagon) and the dashed one depict the set of plaquettes act simultaneously on both subsystems.

the number of plaquettes crossed by the one edge of the hexagon be n . Now we can enumerate the number of plaquettes which acting on A : $\Sigma_A = 3n(n-1)+1$ and the total number of spins of the subsystem A is: $6n^2$. There are $\Sigma_{AB} = 6n$ plaquettes which act between A and B . Let the system be in the state $|0000\rangle$. With these realizations of the subsystems and since $|P| = \Sigma_A + \Sigma_B + \Sigma_{AB}$ we can turn on to calculate the entanglement entropy between two subsystems:

$$S_A = \log 2^{\Sigma_{AB}-2} = \Sigma_{AB} - 2 = 6n - 2 \quad (31)$$

We can relate this entropy to the perimeter of the subsystem A by choosing the height of a plaquette as unit. By this the perimeter of A is: $\partial A = 6n$ and the entropy then reads:

$$S_A = \partial A - 2 \quad (32)$$

Generally for a irregular lattice the entropy for a convex shape will be: $S_A = \kappa \partial A - \gamma$ where the coefficient κ is a nonuniversal depending on the shape of the region while the constant $\gamma = 2$ will be universal and has a topological nature. So we see that the entanglement entropy for the topological color code scales with the boundary of the subsystem which is a manifestation of so called *area law*^{11,19,20}.

This latter relation for the entanglement entropy is consistent with derivation of A. Kitaev *et al.*¹² and M. Levin *et al.*¹³ where they proposed for a massive topological phase there is a topological subleading term for the entanglement entropy which is related to the quantum dimension of the abelian phase. The total quantum dimension for the topological color code will be:

$$\gamma = \log \mathcal{D} \quad \mathcal{D} = 4 \quad (33)$$

The quantity \mathcal{D}^2 is the number of topological superselection sectors of abelian anyons. For Kitaev's toric code there are only four such sectors leading to $\gamma = \log 2$. So the total quantum dimension in the topological color code is bigger than the toric code. The abelian phase of the toric code is characterized via appearing a global phase for the wavefunction of the system by winding an electric (magnetic) excitation around a magnetic (electric) excitation¹². In the case of color code the excitations are colored and they appear as end points of open colored strings of a shrunk lattice¹⁶. Winding a colored X -type excitation around the Z -type one with different color gives an overall factor $(-)$ for the wavefunction of the model, i.e the phase is abelian. Therefore the contribution of the color to the excitations makes the abelian phase of the color code richer than the toric code with a bigger quantum dimension.

Now let the system be in a generic state such as Eq.(21). The reduced density matrix then reads:

$$\rho_A = \sum_{ijkl,mnpq} a_{ijkl} \bar{a}_{mnpq} \text{Tr}_B(X_1^i X_2^j X_3^k X_4^l \rho_0 X_1^m X_2^n X_3^p X_4^q) \quad (34)$$

Some remarks are in order. For two different nontrivial closed string operators but with the same homology and color, say them X and X' , they will have same support and are related via a trivial closed string $g \in G$, i.e $X' = gX$. Since $[g, X] = 0$, two string will have the same effect on the ρ_0 , i.e. $X' \rho_0 = gX \rho_0 = X \rho_0$. We can exploit this property of string opera-

tors in order to choose the strings appearing in Eq.(34) in which that they do not cross subsystem A . Indeed the strings X_i act only on the subsystem B , i.e $X_{iA} = \mathbf{I}_A$. This leads to $\text{Tr}_B(X_i \rho_0 X_i) = \text{Tr}_B(\rho_0)$ for $i = 1, 2, 3, 4$ and $\text{Tr}_B(X_1^i X_2^j X_3^k X_4^l \rho_0 X_1^i X_2^j X_3^k X_4^l) = \text{Tr}_B(\rho_0)$ for $i, j, k, l = 0, 1$. Other cases will be zero. To clarify this, let for example consider the simple case $\text{Tr}_B(X_1 \rho_0)$:

$$Tr_B(X_1\rho_0) = \sum_{g,g' \in G} g_A|0_A\rangle\langle_A 0|g'_A \sum_{g''_B} \langle_B 0|g''_B X_A g_B|0_B\rangle \langle_B 0|g'_B g''_B|0_B\rangle = \sum_{g,g' \in G} g_A|0_A\rangle\langle_A 0|g'_A \langle_B 0|g'_B X_B g_B|0_B\rangle \quad (35)$$

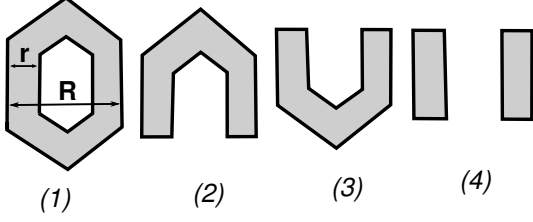


FIG. 4: (color online) Different bipartition of the lattice in order to drop the bulk and boundary effect through the definition of topological entanglement entropy.

On the other hand from the group property $g' = g\tilde{g}$ the above expression becomes:

$$Tr_B(X_1\rho_0) = \sum_{g,\tilde{g} \in G} g_A|0_A\rangle\langle_A 0|g_A\tilde{g}_A \langle_B 0|\tilde{g}_B X_B|0_B\rangle \quad (36)$$

Which implies that $\tilde{g}_B = X_B$, otherwise the above expression will become zero. The fact $\tilde{g} = \tilde{g}_A \otimes \tilde{g}_B \in G$ explicitly implies that the operator \tilde{g}_A must be a non-contractible strings which is impossible since it must act solely on A . So we will leave with $Tr_B(X_1\rho_0) = 0$. The same arguments may also apply for other cases. Finally the entanglement of a convex region for a generic state will become:

$$\rho_A = Tr_B(\rho_0) \quad , \quad S_A = \partial A - 2 \quad (37)$$

J. Topological Entanglement Entropy

As we see from the Eq.(32) there exists a subleading term with topological nature. This is a characteristic signature of existing topological order which has been found on the subleading term of the entanglement entropy. To be more precise on the topological character of subleading term, we can construct a set of bipartitions in which the boundary contribution is dropped and remaining term is stemmed from the topological nature of the code and inspire the topological order. To drop the bulk and boundary degrees of freedom we consider a set of partitions which has been shown in Fig.(4). Topological entanglement entropy then arises from the following combination of entanglement entropy:

$$S_{topo} = \lim_{R,r \rightarrow \infty} (-S_{1A} + S_{2A} + S_{3A} - S_{4A}) \quad (38)$$

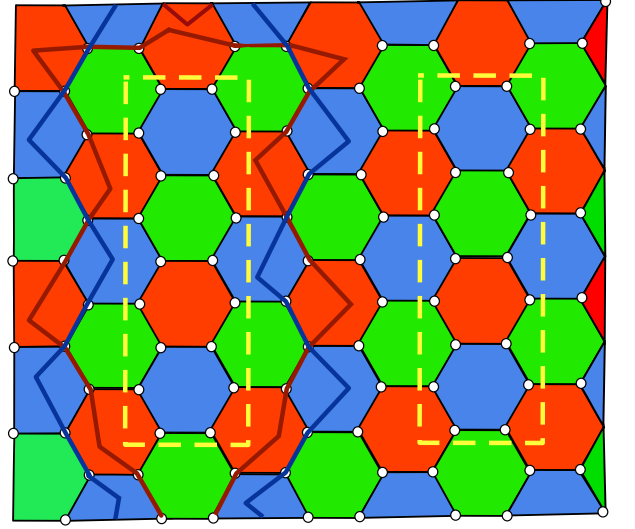


FIG. 5: (color online) One of subsystems, say A , composed of two disjoint regions which introduce some nontrivial colored closed string acting solely on B .

For each bipartition one can use the entanglement entropy as before, namely: $S_G = \log(|G|) - \log(d_A d_B)$. Up to now the cardinalities d_A and d_B were determined by the number of plaquette operators acting solely on A and B , respectively as: $d_A = 2^{\Sigma_A}$ and $d_B = 2^{\Sigma_B}$, where Σ_A and Σ_B stand for the number of plaquette operators acting only on A and B , respectively. However for calculating of the S_{topo} we should care about the counting of them. For the case in which each partition is a single connected region (for example bipartitions (2) and (3) in Fig.(4)) the previous arguments work, but for disjoint regions such as (1) and (4) in Fig.(4) we should extend the above result. As an example a simple case has been shown in Fig.(5) where we have supposed the subsystem A is composed of two disjoint regions (two dashed rectangles which we realize them as A_1 and A_2) while the subsystem B is a single connected one. By inspection we see that product of two set of plaquettes, say blue and green ones, which act on A_1 and the ones acting simultaneously on A_1 and B will result a red string which acts only on B . The same scenario can be applied for other choices of the plaquettes, e.g. red and green or red and blue, which yield blue and green string leaving A_1 . But as we pointed out before one of them will be immaterial since there is an interplay between homology and color. The main point is that it is not possible to produce these colored closed strings which act only on B from the prod-

uct of the plaquettes of region B . The same thing will be held for the other disjoint regions of A , say A_2 . So we have a collection of closed strings with nontrivial effect on B and we must take into account them in calculation of d_B . But a remark is in order and that if for example we combine two red strings, the resultant is not a new closed string because we can produce these two red string from the product of the blue and green plaquettes of region B . Therefore for the case shown in Fig.(5) there are only two independent closed strings of this type with a nontrivial effect on B . With these remarks, now the cardinalities d_A and d_B read:

$$d_A = 2^{\Sigma_A} \quad , \quad d_B = 2^{\Sigma_B+4-2} \quad (39)$$

We can generalize the above results. Let the partitions A and B are composed of m_A and m_B disjoint regions, so the cardinalities will be:

$$d_A = 2^{\Sigma_A+2m_B-2} \quad , \quad d_B = 2^{\Sigma_B+2m_A-2} \quad (40)$$

Now we move on in order to calculate the topological entanglement entropy defined in Eq.(38). For the partitions shown in Fig.(4) we have:

$$m_{1B} = m_{4A} = 2$$

$$m_{1A} = m_{2A} = m_{2B} = m_{3A} = m_{3B} = m_{4B} = 1 \quad (41)$$

$$\Sigma_{1A} + \Sigma_{4A} = \Sigma_{2A} + \Sigma_{3A} \quad (42)$$

Finally the topological entanglement entropy then reads as follows:

$$S_{topo} = -4 \quad (43)$$

Topological entanglement entropy depend only on the topology of the regions and no matter with their geometries¹². This derivation for topological entanglement entropy of color codes is consistent with the sub-leading term of scaling of the entropy. The topological contribution to the entanglement entropy is $S_{topo} = -2\gamma$ ¹². This leads to $\gamma = 2$ a something which has also been derived Eq.(32).

V. ENTANGLEMENT PROPERTIES OF PLANAR COLOR CODES

An important class a topological stabilizer codes in practice is planar codes which are topological codes that can be placed in a piece of planar surface. These planar codes are very interesting for topological quantum

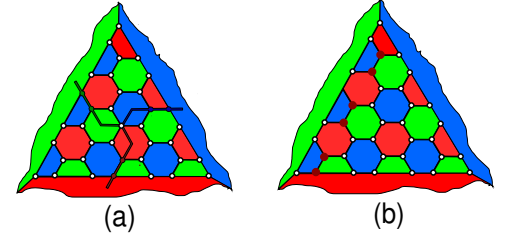


FIG. 6: (color online) A class of color code on the plane. It includes borders each of one color. (a) 3-string net commutes with all plaquettes operators and make a remarkable feature of quantum entanglement distillation (b) A manifestation of colored string as a bipartition.

memory and quantum computations^{9,15}. A planar color code will obtain from a color code without border when a couple of plaquettes removed from the code. For example when a plaquette, say green, is removed only green string can have endpoint on the removed plaquette not the blue and red strings. The same scenario holds for other plaquettes. By this construction we will end with a color code that has three border each of one color. To each border only strings can have endpoint which have same color of that border. The most important of such planar color code is *triangular code* that has been shown in Fig.(6). The essential properties of such code is determined via realizing a 3-string operator and its deformation. We denote them by T^X and T^Z so that $\{T^X, T^Z\} = 0$ since they cross each other once at string of different colors. This latter anticommutation relation makes the triangular color code very interesting allowing a full implementation of the Clifford group¹⁵. Instead of giving such fruitful properties, we are interested to the entanglement properties of the triangular code.

To have a concrete discussion, we consider a triangular code which contains hexagons like what has been shown in Fig.(6). The total number of plaquettes and vertices are $|P| = \frac{3}{2}k(k+1)$ and $|V| = 3k(k+1) + 1$, respectively, where k in an integer number. The plaquettes operators like what defined in Eq.(1) have been used in order to obtain a stabilizer structure for this code. A main point about the planar code is that there are no constraints on the action of plaquettes operators. For example if we product all red and green plaquettes the resulting operator will not leave the code invariant, a property that was absent for color code on compact surface. In fact the product of plaquettes have non-trivial action at the edges of the triangular. The coding space will span with the states which are fixed points of all plaquettes operators. With the above identifications for the number of plaquettes and vertices the dimension of the coding space will be: $\Lambda = \frac{2^{|V|}}{2^{|P|}2^{|P|}} = 2$ which shows triangular code encodes single qubit. Two states are completely determined by the elements of stabilizer group and 3-string operator. Note that here 3-string operator plays the role like nontrivial strings in the color code on the torus. For

triangular code the 3-string is nontrivial, i.e. it commutes with all plaquette operators and is not products of some plaquettes. So the stabilized states will be:

$$|0\rangle = |G|^{-1/2} \sum_{g \in G} g|0\rangle \otimes |V|, \quad |1\rangle = T^X |0\rangle \quad (44)$$

A generic state can be made of superposition of above states such as: $|\psi\rangle = \sum_{i=0}^1 a_i |i\rangle$ where $\sum_{i=0}^1 |a_i|^2 = 1$. The reduced density matrix in Eq.(11) gives the thing which we need to evaluate the entanglement entropy. Again we make different bipartitions and calculate the entanglement entropy.

Let the system be in the state $|0\rangle$. A single qubit is maximally entangled with rest of the system while two qubits are not entangled implying that the triangular code is also a multipartite entangled structure. As another bipartition we consider a color spin chain such like red chain in Fig.(6b). This string contains $2k$ qubits and anticommutes with one of the plaquettes which the string has an endpoint on it, i.e. they share in a single qubit, thus its action on the coding space gives rise to errors or on the other hand to the appearance of excitations above the ground state if we adopt the coding space as ground state of a local Hamiltonian as in Eq.(10). However such a string has maximal entanglement $S_A = 2k$ with other qubits of the code. This means that all configurations of the spin chain are allowed in the state $|0\rangle$ of the code, a feature that was absent in the topological color code on the torus where only configurations with even number of spin flipped were allowed in the state of the code (see Eq.(18)).

Taking into account the qubits living on the 3-string net as subsystem A leads to occurrence of configurations of subsystem A with an only even number of spin flipped in the state $|0\rangle$. For this string net as shown in Fig.(6a) the number of qubits of the string is $2k+1$, and the entanglement entropy then will become: $S_A = 2k$. By inspection we see that the action of the plaquettes operators flips only even number of qubits of the string net. Now let the system be in a generic state such as $|\psi\rangle$. All possible configurations of string net are allowed since all of them can be realized by applying some 3-string operators T^X . There are 2^{2k} configurations with even number of spin flipped and 2^{2k} configurations with odd number of spin flipped. The states $|0\rangle$ and $|1\rangle$ include even and odd configurations, respectively. Therefore the entanglement entropy for a generic state will be: $S_A = 2k + H(\alpha)$ where $\alpha = |a_0|^2$.

What about the topological entanglement entropy? In order to answer this question we obtain a set of bipartitions such as in Fig.(4) in a large triangular code. Let as before Σ_A and Σ_B stand for the number of plaquettes acting only on A and B , respectively and Σ_{AB} account the number of plaquettes acting simultaneously on A and B . All plaquettes operators are independent. To get things simply let consider a simple case where the subsystem A is a single convex connected region. The cardinality

of the subgroup G_A is 2^{Σ_A} . However there are two non-trivial closed strings acting on subsystem B which is impossible to provide them by products of some plaquettes of B . In fact these two independent strings are resulted from the products of some plaquettes, say red and green, which are free to act on A . So the cardinality of the subgroup B reads: 2^{Σ_B+2} . Thus for the entanglement entropy we provide: $S_A = \Sigma_{AB} - 2$.

In order to calculate the topological entanglement entropy first for different bipartitions the entanglement entropy is calculated and then the expression in Eq.(38) gives the topological entropy. For a disconnected region like (1) or (4) in Fig.(4) the constraint we imposed in Eq.(40) is no longer true for the present case of triangular code. For the bipartition (1) in Fig.(4) the cardinalities of subgroups G_A and G_B will be $d_A = 2^{\Sigma_{1A}+2}$ and $d_B = 2^{\Sigma_{1B}+2}$, respectively. However for the bipartitions (4) in Fig.(4) the cardinalities will be $d_A = 2^{\Sigma_{4A}}$ and $d_B = 2^{\Sigma_{4B}+4}$, respectively. Thus the topological entanglement entropy becomes: $S_{topo}^t = -4$. Although the closed string structures of bipartitions in the triangular code due to the boundary effects differ from the color code on the torus, the topological entanglement entropy is same for both systems, a fact that is related to the fact that both structures have the same symmetry.

VI. CONCLUSIONS

In this paper we calculated the entanglement properties of two-dimensional topological color codes (TCC). The entanglement entropy was measured by the von Neumann entropy. We considered two structures of TCC either defined on the compact or planar surface. The coding space of TCC is spanned by a set of states in which are the fixed points of a set of commuting Pauli operators. In fact this set stabilizes the coding space, and is formed by a set of generators that are plaquettes operators of the code. Product of different plaquettes produces colored strings which in fact are the closed boundary of some plaquettes. However, there exist some independent non-trivial strings winding the handles of manifold where the model defined on with the property that they commute with the plaquettes operators but are not in the stabilizer group. These nontrivial strings make remarkable properties of the color code more pronounced.

For a manifold with genus g , the coding space spanned by 4^{2g} states that can be set in which be ground state of a Hamiltonian. The degeneracy of ground state depends on the genus of the manifold, a feature of topological order. Different states of ground space can be constructed by means of elements of spin flipped stabilizer group. In order to calculate the entanglement properties of the TCC, the reduced density matrix of a subsystem is provided by tracing over remaining degrees of freedom. We did this by using the group properties. For both structures of color code either on compact

or planar surface while a single qubit is maximally entangled with others, two qubits are no longer entangled. This finding manifests the color code is a genuinely multientangled structure. We also considered other bipartitions such as spin chains, spin ladders with various colors and homologies. For all bipartitions we find the entanglement entropy depend on the degrees of freedom living on the boundary of two subsystems. However in the entanglement entropy of a convex region, there is a term which is ascribed to the topological properties of region not the geometry, a feature that also arises in a massive topological theory¹². The fact that for a region of structure the entanglement entropy scales with the boundary is a feature of *area law* which is also of great interest in other branch of physics such as black holes²¹.

We exploited the scaling of the entropy to construct a set of bipartitions in order to calculate the topological entanglement entropy. We find that it is twice than the topological entropy in the topological toric code. The non-vanishing value for topological entanglement and dependency of degeneracy on the genus of the surface demonstrate remarkable features on the fact that topological color code maybe fabric to show topological order. For the toric code model the total quantum dimension of excitation is 4 which stands for different superselection or its anyonic excitations. The total quantum dimension of color code is 16 inspiring that the topological color codes may carry richer anyonic

quasiparticles. They may be colored and their braiding will have nontrivial effect on the wavefunction of the system. Indeed braiding of a colored quasiparticle around the another one with different color will give rise to global phase for the wavefunction, i.e they are abelian excitations. Triangular color code with a remarkable application for entanglement distillation is also a highly entangled code. Although the colored strings employed in the 2-colex in the compact surface are not relevant in the triangular code, the notion of string-net gives some essential properties to the triangular code. In the state of the triangular code all configurations of a colored string, say a red one in Fig.(6b), are allowed, i.e is has maximal entanglement with the rest of the system. However, for a string-net only the configurations with even number of spin flipped are allowed. Entanglement entropy scales with boundary of the region and involves a topological term. This topological terms yields a non-vanishing topological entanglement entropy which is same with what we obtained for the 2-colex on the torus.

Fruitful discussions and comments with Dr. A. Langari are acknowledged.

References

-
- * kargarian@physics.sharif.edu
 - ¹ S. Oh and J. Kim, Phys. Rev. B **71**, 144523 (2005).
 - ² V. Vedral, New J. Phys **6**, 102 (2004).
 - ³ X. G. Wen, Phys. Lett. A **300**, 175 (2002).
 - ⁴ L. Amico, R. Fazio, A. Osterloh, and V. Vedral, Rev. Mod. Phys. **80**, 517 (2008).
 - ⁵ N. Goldenfeld, *lectures on phase transitions and the renormalization group*, Westview Press, 1992.
 - ⁶ X. G. Wen and Q. Niu, Phys. Rev. B **41**, 9377 (1990); X.G.Wen, Phys. Rev. Lett. **90**, 016803 (2003).
 - ⁷ A. Y. Kitaev, Ann. Phys. (N.Y.) **303**, 2 (2003).
 - ⁸ D. Gottesman, Phys. Rev. A **54**, 1862 (1996).
 - ⁹ E. Dennis, A. Kitaev, A. Landahl and J. Preskill, J. Math. Phys. **43**, 4452 (2002).
 - ¹⁰ A. Hamma, R. Ionicioiu, and P. Zanardi, Phys. Rev. A **71**, 022315 (2005); A. Hamma, R. Ionicioiu, and P. Zanardi, Phys. Lett. A **337**, 22 (2005).
 - ¹¹ S. Ryu and T. Takayanagi, arXiv:hep-th/0605073.
 - ¹² A. Kitaev and J. Preskill, Phys. Rev. Lett. **96**, 110404 (2006).
 - ¹³ M. Levin and X. G. Wen, Phys. Rev. Lett. **96**, 110405 (2006).
 - ¹⁴ H. Bombin, M. A. Martin-Delgado, Phys. Rev. Lett, **97**, 180501 (2006).
 - ¹⁵ H. Bombin, M. A. Martin-Delgado, Phys. Rev. A, **76**, 012305 (2007).
 - ¹⁶ H. Bombin, M. A. Martin-Delgado, Phys. Rev. B, **75**, 075103 (2007).
 - ¹⁷ R. Raussendorf, S. Bravyi, J. Harrington, Phys. Rev. A, **71**, 062313 (2005).
 - ¹⁸ W. K. Wootters, Phys. Rev. Lett, **80**, 2245 (1998).
 - ¹⁹ M. B. Plenio, J. Eisert, J. Dreißig, and M. Cramer, Phys.Rev.Lett. **94**, 060503 (2005).
 - ²⁰ R. Bousso, Rev. Mod. Phys. **74**, 825 (2002).
 - ²¹ S. Ryu and T. Takayanagi, Phys. Rev. Lett. **96**, 181602 (2006).